and they may have evolved, on average, two to three times as rapidly. Analysis of the possible significance of this difference is a complex problem. Different long-term rates for invertebrates and vertebrates may reflect differences in intrinsic evolutinary potential (as a function of population structure, generation length, and so forth) or extrinsic environmental factors.

Kurtén's (*4*) conclusion that rates of morphological evolution in Quaternary (Pleistocene and post-Pleistocene) mammals exceeded those in Tertiary mammals is also based on comparison of rates measured over different intervals of time. Kurtén's mean value for Tertiary rates is predicted almost exactly by a regression of his Quaternary rates on temporal interval, indicating that Quaternary and Tertiary rates are not significantly different.

Finally, we can address the question of how rates of phyletic evolution measured over long intervals of geological time relate to rates characteristic of speciation and adaptive radiation on shorter time scales, a point crucial in the argument that ordinary microevolutionary processes cannot explain macroevolutionary events observed in the fossil record (*5*). Rates on the order of 60,000 d in laboratory selection experiments (Table 1 and domain I in Fig. 1) were sustained for only a few years; they exceed homeostatic limits (*9*) and exceed rates to be expected in nature. Rates observed during colonization of new or empty adaptive zones average about 400 d (domain II); all populations studied were viable, and rates on the order of 400 d probably characterize speciation and radiation in new adaptive zones. Post-Pleistocene rates (domain III) average about 4 d in integrated coevolved faunas, while rates measured over longer intervals in the fossil record (domain IV) average less than 1 d. These low rates are measured over such long temporal intervals that differences in morphology are swamped by interval length, and net change greatly underestimates total change. Microevolutionary rates measured on a scale of tens or hundreds of years are much higher than phyletic rates derived from fossils. A microevolutionary rate of 400 d is sufficient to change a mouse into an elephant in 10,000 years. However, the stratigraphic record is rarely complete enough on a scale of hundreds or even thousands of years to preserve such a rapid transition (*10*). Evolution on a microevolutionary scale is invisible in the fossil record, but this does not preclude microevolutionary processes operating over geological time from producing macroevolutionary change on the longer time scale. Microevolution and macroevolution are different manifestations of a common underlying process.

Rates of evolution measured over different intervals of time cannot be compared without appropriate temporal scaling. This conclusion is based on comparative study of morphological rates, but it holds in principle for rates of taxonomic and molecular evolution as well.

PHILIP D. GINGERICH
Museum of Paleontology,
University of Michigan,
Ann Arbor 48109

References and Notes

1. G. G. Simpson, *Tempo and Mode in Evolution* (Columbia Univ. Press, New York, 1944), p. 3; *The Major Features of Evolution* (Columbia Univ. Press, New York, 1953), p. 3.
2. L. Van Valen, *Evol. Theory* **1**, 1 (1973); S. M. Stanley, *Syst. Zool.* **22**, 486 (1973).
3. L. Van Valen, *Nature (London)* **252**, 298 (1974).
4. B. Kurtén, *Cold Spring Harbor Symp. Quant. Biol.* **24**, 205 (1960).
5. S. M. Stanley, *Proc. Natl. Acad. Sci. U.S.A.* **72**, 646 (1975); *Macroevolution: Pattern and Process* (Freeman, San Francisco, 1979), p. 63.
6. J. B. S. Haldane, *Evolution* **3**, 51 (1949).
7. J. T. Bonner, *Paleontol. Soc. Mem.* **2**, 1 (1968).
8. F. L. Bookstein, P. D. Gingerich, A. G. Kluge, *Paleobiology*. **4**, 120 (1978).
9. I. M. Lerner, *Genetic Homeostasis* (Oliver and Boyd, Edinburgh, 1953), p. 8; D. S. Falconer, *Quantitative Genetics* (Longman, London, 1981), p. 170.
10. D. E. Schindel, *Paleobiology* **6**, 408 (1980); P. M. Sadler, *J. Geol.* **89**, 569; P. D. Gingerich, *Proc. Third N. Am. Paleont. Conv., Montreal* **1**, 205 (1982); P. M. Sadler and L. W. Dingus, *ibid.* **2**, 461 (1982).
11. Rates based on comparison of areal or volumetric measurements or counts are included in a few instances. These were divided by their dimensionality (2 or 3, respectively) to make them comparable to linear rates.
12. E. H. Ashton and S. Zuckerman, *Proc. Roy. Soc. London* **137**, 212 (1950); **138**, 204 (1951); R. J. Berry, *Evolution* **18**, 468 (1964); R. F. Johnston and R. K. Selander, *ibid.* **25**, 1 (1971); J. L. Patton, S. Y. Yang, P. Myers, *ibid.* **29**, 296 (1975).
13. J. B. Foster, *Occas. Pap. Brit. Columbia Prov. Mus.* **14**, 55 (1965); L. R. Heaney, *Evolution* **32**, 29 (1978).
14. A. Hallam, *Nature (London)* **258**, 493 (1975).
15. E. H. Colbert, *Evolution* **2**, 145 (1948); R. S. Bader, *ibid.* **9**, 119 (1955); B. Kurtén, *Acta Zool. Fenn.* **90**, 37 (1955); T. Downs, *Los Angeles County Mus. Contrib. Sci.* **45**, 62 (1961); V. J. Maglio, *Trans. Am. Phil. Soc.* **63**, 105 (1973); L. G. Marshall and R. S. Corruccini, *Paleobiology* **4**, 101 (1978); P. D. Gingerich, *Annu. Rev. Earth Planet. Sci.* **8**, 407 (1980).
16. I thank W. Atchley, C. Badgley, M. Bell, A. Boucot, F. Bookstein, B. Chernoff, P. Dawson, W. Fink, D. Fisher, D. Futuyma, C. Gans, P. Grant, L. Heaney, F. Jenkins, P. Myers, J. Patton, L. Radinsky, B. H. Smith, and R. Sokal for reading the manuscript. A. Kluge and G. R. Smith also contributed to development of the ideas presented here. Karen Klitz drew Fig. 1. Supported by NSF grant DEB 82-06242.

27 January 1983; revised 4 April 1983

Solar System Ice: Amorphous or Crystalline?

Abstract. *The role of meteoritic bombardment on icy surfaces in the solar system is investigated. Using recent theoretical results concerning the nature of ejecta from impact craters in ice, the author concludes that the ratio of amorphous to crystalline ice surfaces should be lower than 1.0.*

The discovery of many partially or totally ice-covered satellites of the giant planets and the well-known presence of ice on the rings of Saturn and in cometary nuclei have prompted questions about the structure of this ice. It is assumed here that water ice, which is presumably the main constituent, is not much influenced by the addition of other types of ice. Exceptions are ice-ammonia solutions which have a significantly lower melting temperature and the clathrates. Golitsyn (*1*) drew attention to the process of slow deformation of ice in the crust of satellites, which may lead to tectonic phenomena resembling those on the earth. Reynolds and Cassen (*2*) concluded that radioactive heating may permit convective motions of ice corresponding to Rayleigh numbers between 10^3 and 10^6 and that the ice should be crystalline because the temperature in the interior would be higher than 150 K, which is the upper limit for the existence of amorphous water ice. On the other hand, Klinger (*3*) suggested that ice in the interior of some satellites could be amorphous and that its slightly exothermic behavior during heating below 150 K by radioactive and tidal effects may produce sufficient heat to melt and resurface satellites such as Enceladus. This mechanism may be valid if the ice contains enough NH_3 to lower its melting temperature considerably. This report focuses on the meteoritic bombardment of icy surfaces and, in particular, on the formation of amorphous ice with its significantly different thermal, mechanical, and optical properties. These differences may be observable.

Cratering impacts in ice. Impacts that lead to plastic deformation and fragmentation both of the projectiles and of the target materials are difficult to treat theoretically because the fracture mechanism and fracture resistance are not bulk properties but structure-sensitive properties of solids. These properties depend on the microscopic perfection of the solids, and thus their evaluation requires making drastic approximations on the basis of experimental data. Inasmuch as ice has seldom been studied both as a target and as a projectile, not many facts are available with which to make suitable generalizations. The main questions concern the size of the craters, the amount

and velocity of the ejecta, and whether these ejecta are solid, liquid, or gaseous. For ice, the last problem is particularly important because of its low melting temperature and ease of vaporization.

A theory and a numerical code have been proposed (*4, 5*) that permit satisfactory general treatment of these phenomena, especially for rocks. Croft (*6*) developed a semianalytical version of these procedures that involves the gamma model of crater formation, in which a spherical isobaric core is centered just below the point of impact, while beyond the core the pressure drops off as $r^{-\gamma}$, where r is distance from the core. With suitable experimental data the various adjustable parameters can be determined. Croft obtained quantitative results for iron, rock (gabbroic anorthosite), and ice projectiles impinging on an ice target with velocities ranging from 2 to 55 km/sec. From these results, one can evaluate the ratio of the volume of the melted and vaporized ice target to the volume of the projectile. This ratio is a somewhat less than exponentially increasing function of velocity (Fig. 1). The curve for ice projectiles intersects those for iron and rock because an ice projectile itself melts and vaporizes, making a contribution significant at low velocities. Figure 2 shows the ratio of vaporized to melted ice at the moment the crater is formed by projectiles moving at various velocities. No vaporization occurs at velocities less than 4 to 6 km/sec; for velocities greater than 10 km/sec the ratio of vapor to water is about 0.4. For small craters, produced by velocities greater than about 10 km/sec, most of the ejecta are solid; for craters around 100 km the fraction of solids is about 0.5; and for craters larger than a few hundred kilometers, most of the ejecta are liquid or vapor (*6*).

An additional source of water vapor is the rapidly evaporating water droplet ejecta. A quantitative estimate of this process would require knowledge of the size distribution of these droplets. A rough estimate (*6*) suggests, however, that 10 to 30 percent of the ejected water quickly evaporates, increasing the total ratio of vapor to water to perhaps 0.8.

Phase transformations. Hexagonal water ice is unstable at pressures above 2 kbar. There are many high-pressure phases at temperatures below about 250 K, so pressures produced during impact can lead to the formation of various phases that, at the ambient temperature, may remain in a stable or metastable state after impact. These processes were investigated in detail by Gaffney and Matson (*7*), who concluded that the high-pressure polymorphs of ice should be ubiquitous on bodies in the solar system.

Besides the polymorphic stable phases, ice formed by direct condensation of water vapor below about 150 K is amorphous (*8, 9*). Solidification of liquid water always leads to the usual crystalline hexagonal ice. There are two kinds of amorphous ice: a denser one below about 10 K and a more common, less dense amorphous ice above that temperature. With increasing temperature, amorphous ice gradually evolves some heat, mostly connected with shrinkage, but it is not until 150 or 153 K that a rapid phase change occurs into a crystalline cubic form. Cubic ice itself is, however, metastable, and near 200 K it transforms

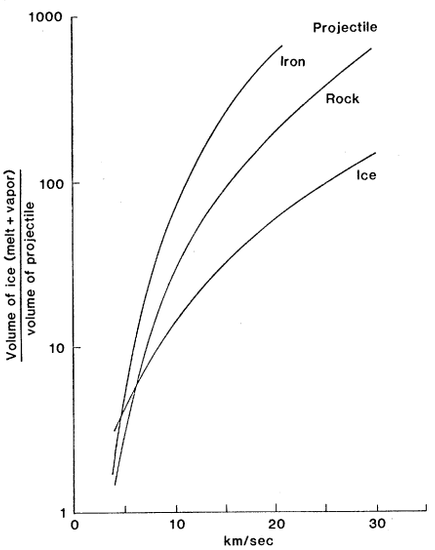

Fig. 1. Ratio of the volume of nonsolid ejecta from ice to the volume of iron, rock, or ice projectiles as a function of velocity [based on the data of Croft (*6*)].

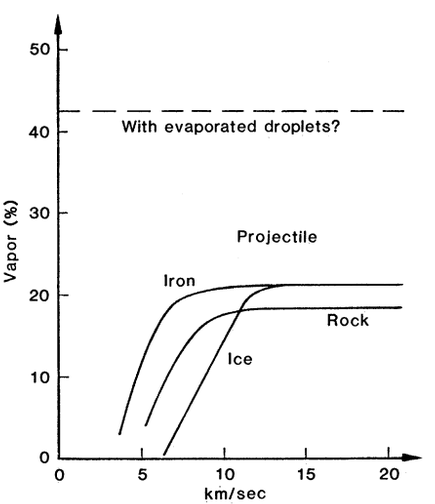

Fig. 2. Ratio of vaporized to melted ice as a function of velocity for various projectiles [based on the data of Croft (*6*)].

into the usual hexagonal ice. During the irreversible transformation at 153 K, 10^9 ergs per gram of ice is rapidly released, raising its temperature by 37 K. Thus, when an impact occurs on amorphous rather than crystalline ice, the heat of crystallization increases the energy available to melt the ice. It turns out, however, that this additional energy makes a significant contribution only at velocities below about 1 km/sec, at which, according to the findings of Croft (*6*), all ejecta should be solid.

In considering impacts on amorphous ice, other factors should be taken into account besides the exothermic heat. The two most important ones are thermal conductivity (one or two orders of magnitude lower) and the suppression of plastic deformation of amorphous as compared to crystalline ice. From studies of the effects of irradiation in solids, (*10*) it is known that—if other factors are about the same—the much lower thermal conductivity would limit the spread of the evolved heat and thus lead to higher local temperatures. As a result, the ratio of water vapor to liquid water should be higher.

The role of limited plastic deformation is difficult to assess without experimental data. The ratio of impact energy to crater size depends on the strength of the target material for small craters and on gravity for larger craters. On the earth the strength-gravity transition occurs at a crater diameter of about 1 m, while on Mimas it may be as large as 1 km (*11*). A scaling relation (*12*) indicates that, if all other factors are kept constant, the volume of a small crater can be assumed to be roughly proportional to the reciprocal of the strength of the target material. While no data are available on the mechanical strength of amorphous ice, one can use the analogy of vitreous and crystalline silicas, which have been well investigated (*13*). Using data for that system, one concludes that the impact strength of amorphous ice is perhaps four times lower than that of crystalline ice, and thus one can expect strength-controlled craters in amorphous ice to be larger.

Icy surfaces. The maximum impact velocity of meteorites on a body in the solar system is determined not only by the sun's gravity but also by that of the body itself and by the body's orbital velocity. For the earth, the maximum impact velocity is 72 km/sec, while for the satellites of Jupiter and Saturn one obtains around 56 and 40 km/sec (the most likely values being around 40, 18, and 14 km/sec, respectively). These impacts may produce crystalline ice

polymorphs in the impact craters (*7*). As mentioned above, the water component of the impact's ejecta will partly evaporate and the rest will freeze on the surface, producing normal crystalline hexagonal ice. The vapor component will partly escape into space and partly condense as amorphous ice on the numerous solid ejecta and around the craters. Condensation on solid ejecta is very important because most meteorites, and thus most craters, are small, and it is the small craters for which more than half the ejecta are solid.

It appears that ice freshly formed on the surfaces of icy bodies by meteoritic bombardment should be partly crystalline and partly amorphous, the ratio of the two depending on the ratio of solidified liquid water to condensed water vapor and on the fraction of solid ejecta. In view of the various uncertainties discussed above, one can only say that less than 50 percent of the volume of the bombarded icy layer should be amorphous. This conclusion should be modified for the rings of Saturn because they are probably continuously recovered by condensation of water molecules sputtered from the outer edge of the A ring (*14*). The conclusion could be checked by observing the sun through the rings from a spacecraft: the ring particles collide and produce interparticle dust (*15*) that, in analogy to observations from the earth, should lead to a halo at 22° and 47° if the dust is crystalline and to no halos if it is amorphous.

It appears possible, in most cases, to distinguish between the various polymorphs of crystalline ice on satellites (*7*). On the other hand, the problem of identifying amorphous ice is difficult because the optical differences are usually limited to the shape of the reflection lines at 3 and 13 μm. In principle, amorphous ice on a satellite could be identified if, in analogy to the early studies of our moon, it were possible to deduce the thermal inertia $(k\rho c)^{1/2}$ of the satellite's surface by observing the rate of temperature change near the terminators (*16, 17*). The thermal conductivity of amorphous ice k at 20 K is 10^3 times and at 150 K more than 10 times lower than that of hexagonal ice (*3*), while the density ρ is essentially the same and the specific heat c in the pertinent range of temperatures should differ very little (*18*). It would be necessary, however, to ascertain first that the surface is not a loose aggregate of fine powders, and this may be a very difficult task.

R. SMOLUCHOWSKI
Departments of Astronomy and Physics, University of Texas, Austin 78712

References and Notes

1. G. S. Golitsyn, *Geophys. Res. Lett.* **6**, 446 (1979).
2. R. T. Reynolds and P. M. Cassen, *ibid.* **6**, 121 (1979).
3. J. Klinger, *Nature (London)* **299**, 41 (1982).
4. J. D. O'Keefe and T. J. Ahrens, *Lunar Planet. Sci.* **8**, 3351 (1977).
5. D. L. Orphal, W. F. Bowden, A. A. Larson, P. H. Schultz, *ibid.* **11**, 2309 (1980).
6. S. K. Croft, *Geol. Soc. Am. Spec. Pap. 190* (1983); private communication.
7. E. S. Gaffney and S. L. Matson, *Icarus* **44**, 511 (1980).
8. J. A. Ghormley, *J. Chem. Phys.* **48**, 503 (1968).
9. A. H. Narten, C. G. Venkatesh, S. A. Rice, *ibid.* **64**, 1106 (1976).
10. G. J. Dienes and G. H. Vineyard, *Radiation Effects in Solids* (Interscience, New York, 1957).
11. S. K. Croft, *Lunar Planet. Sci.* **13**, 131 and 135 (1982).
12. K. A. Holsapple and R. M. Schmidt, *J. Geophys. Res.* **87**, 1849 (1982).
13. W. D. Kingery, *Introduction to Ceramics* (Wiley, New York, 1960).
14. R. Smoluchowski, *Science* **201**, 809 (1978).
15. ———, *Icarus* **54**, 263 (1983).
16. S. W. Squyres, *ibid.* **44**, 502 (1980).
17. J. R. Spencer, *Lunar Planet. Sci.* **14**, 731 (1983).
18. P. V. Hobbs, *Ice Physics* (Clarendon, Oxford, 1974).
19. I am indebed to Steven Kent Croft for providing him with results of his calculations before publication and for discussions. This research was supported by NASA grant NSG 7505-Suppl. 4.

11 January 1983; revised 20 April 1983

New Burgess Shale Fossil Sites Reveal Middle Cambrian Faunal Complex

Abstract. *Soft-bodied and lightly sclerotized Burgess shale fossils have been found at more than a dozen new localities in an area extending for 20 kilometers along the front of the Cathedral Escarpment in the Middle Cambrian Stephen Formation of the Canadian Rockies. Five different fossil assemblages from four stratigraphic levels have been recognized. These assemblages represent distinct penecontemporaneous marine communities that together make up a normal fore-reef faunal complex.*

The Burgess shale (~ 530 million years old) contains one of the most remarkable fossil faunas in the geological record (*1*). Among its well-preserved fossils are the earliest known representatives of many soft-bodied and lightly sclerotized animal groups (*1*) that together provide a remarkably complete picture of marine life in the Middle Cambrian following the first major radiation of the metazoans (*2*).

The Burgess shale is known essentially from one locality. In 1981 and 1982, new localities of soft-bodied and lightly sclerotized fossils, representing several distinct fossil assemblages, were found. The new localities are in outcrops of the Stephen Formation immediately adjacent to the Cathedral Escarpment. This escarpment is the near vertical margin of a massive dolomitized reef (*3*) that has been traced for 20 km southeast from the Burgess shale locality on Fossil Ridge (*4*). The outcrops are on six mountains: Fossil Ridge, Mount Field, Mount Stephen, Mount Odaray, Park Mountain, and Curtis Peak (Fig. 1).

Up to now, the Burgess shale fossils had been obtained from two levels on Fossil Ridge: the 2.3-m thick Phyllopod bed (*5*) quarried by Walcott between 1910 and 1917, which yielded over 95 percent of the known fossils, and another bed 23 m higher in the section quarried by Raymond in 1930 (*6*). Two communities have been identified in this bed: the benthic *Marrella-Ottoia* community and the poorly represented pelagic *Amiskwia-Odontogriphus* community (*7*). The Raymond quarry bed contains a sparser, less diverse, and less well-preserved assemblage, characterized by the arthropod *Leanchoilia*, the worms *Ottoia* and *Banffia*, and the enigmatic animal *Anomalocaris*.

Few fossils are present in beds closer to the escarpment or in between the quarries. Away from the escarpment, however, in lateral extension of the beds exposed in the Raymond quarry, *Ottoia* occurs in situ, while talus at about this level up to 200 m south of the quarry yielded the arthropods *Sidneyia* and *Leanchoilia* (locality 2, Fig. 1). Most significantly, a number of lightly sclerotized animals, including the arthropods *Proboscicaris*, *Tuzoia*, *Alalcomenaeus*, and the "appendage F" animal (*8*) were found, almost in situ, 65 m above the Walcott quarry, indicating that a fossil-bearing layer is also present at about this stratigraphic level (locality 1, Fig. 1). This level occurs in beds characterized by the trilobite *Ehmaniella burgessensis* (*9*).

The Cathedral Escarpment is most clearly exposed in outcrops on the south face of Mount Field (*4*), about 1.9 km south-southeast of the Walcott quarry (Fig. 1). Among the numerous soft-bodied, lightly sclerotized, and shelly fossils found in uncleaved shales about 30 m west from the reef front (locality 3, Fig. 1) were the rare echinoderm *Echmatocrinus*, which is regarded as the earliest crinoid, and a specimen of the trilobite *Olenoides* with preserved appendages. The presence of *Ottoia* and the sponge